Iron nanoparticle-containing graphene oxide: synthesis and membrane properties

T. Murshudov [a], A. Elshan [a], M. Asadov [a,b], N. Guliyeva [c*], M. Rahimov [d], A. Elsun [e]
[a] *Scientific Research Institute Geotechnological Problems of Oil, Gas and Chemistry, Baku, Azerbaijan*
[b] *Institute of Catalysis and Inorganic Chemistry, Baku, Azerbaijan*
[c] *Baku Engineering University, Baku, Azerbaijan*
[d] *Azerbaijan State Oil and Industry University, Baku, Azerbaijan*
[e] *University of Strasbourg, Institute for Chemistry and Processes for Energy, the Environment and Health, France*

Graphene oxide (GO) layers were obtained by oxidation of graphite. Using iron oxide nanoparticles (FeNP) and GO and by GO reduction, a set of reduced nanocomposites FeNP@GO and FeNP@rGO were obtained. Reduction of GO allowed additional functionalization of active centers in rGO. Control of the properties and structure of the formed nanocomposites was carried out by physicochemical methods (X-ray diffraction (XRD), Fourier transform infrared spectroscopy (FTIR), transmission electron microscopy (TEM), chemical analysis). FeNP@GO and FeNP@rGO nanocomposites were used to remove harmful cations from water.

(Received February 19, 2025; Accepted June 10, 2025)

Keywords: Graphene oxide (GO), Reduced GO (rGO), FeNPs nanoparticles, Composite layers, FeNPs@GO and FeNPs@rGO.

1. Introduction

The development of new functional materials, in particular, based on graphene (G) by modifying the original structure and/or combining two or more nanostructures, is an urgent problem [1]. G derivatives, in particular graphene oxide (GO) and reduced graphene oxide (rGO), are forms of functionalized graphene. The resulting GO and rGO contain oxygen-containing surface groups, including hydroxyl, carboxyl, and epoxy. Depending on the oxidation state, GO and rGO have a non-constant composition [2]. Partially oxidized GO and rGO consist of sp2-bonded carbon atoms in conducting π-states and sp3-hybridized oxidized carbon atoms in non-conducting σ-states [2,3]. The functional groups make GO and rGO hydrophilic and act as reactive centers at the phase interface [3]. The high electronegativity of oxygen atom of GO and rGO materials can adsorb positively charged precursors through electrostatic interactions. This leads to uniform distribution of other active components on GO and rGO with close interface [2,3]. Nanocomposites containing nanoparticles (NPs) incorporate the properties of individual components of nanocomposites based on the graphene system. For example, graphene oxide (GO) nanocomposites, due to their low cost and mass production, are used as membrane materials. This allows the production of materials with improved functionality and potential applications in various fields [4,5]. Studies on the production and analysis of thin-layer graphene oxide have been reviewed in detail [6-15]. Such materials are synthesized in new ways using, for example, metallic NPs [6] and metal oxide NPs [4]. Methods for producing nanocomposites combining iron oxide and graphene oxide or reduced graphene oxide (rGO) are known. In this case, iron oxide NPs can be grown from ionic iron precursors on GO sheets using an autoclave reaction [16]. Methods for producing FeNPs@rGO systems by hydroxide coprecipitation, thermal reaction in organic solvents, and bonding with carboxylate groups of GO

* Corresponding author: rashad.g.abaszade@gmail.com
https://doi.org/10.15251/JOBM.2025.172.119

sheets are also known. The results of a step-by-step synthesis of iron oxide nanoparticles attached to graphene oxide and a study of the properties of the FeNPs@rGO nanocomposite are presented in [17]. The obtained iron oxide and graphene oxide nanocomposites have been used in technological applications [18-22], such as platforms for electrochemical sensing and catalysis [18,28] and as a contrast agent for magnetic resonance imaging [19]. Graphene oxide as a material used is safe for the environment. It has good adsorption properties [23,24]. In this work, for example, we were interested in the efficiency of its use for removing inorganic cation pollutants from wastewater. The aim of this work is to modify the synthesis of FeNPs@GO and FeNPs@rGO composites, as well as to study the filtration properties of the obtained materials for membranes for wastewater treatment from harmful cations.

2. The experimental part

From the analysis of the literature, it follows that graphene oxide is usually obtained by processing graphite powder using strong oxidizing reagents ($KMnO_4$, $NaNO_3$, H_2SO_4) [20,25,26]. This method is safe, provides a low content of inorganic impurities and a small spread of flake sizes. In other words, graphene is obtained by oxidizing graphite, where it undergoes further exfoliation and reduction. Chemical introduction of oxygen groups into graphite expands the interlayer distances of the structure. Such reduction (and exfoliation) of graphite leads to the formation of the graphene structure. The resulting graphene is reduced graphene oxide (rGO), which contains defects and oxygen residues. Functionalization of the GO surface allows modification of its properties. Oxygen groups, especially carboxyl groups, charge GO thin films negatively. Therefore, GO composites can be formed layer by layer by interaction with positively charged particles [27,28]. In this work, the GO surface was functionalized using iron nanoparticles. The information obtained by experimental methods, taking into account the features of obtaining GO nanocomposites, allowed us to study the structural properties and distribution of nanoparticles on GO sheets. Data on the formation of GO layers with the participation of iron nanoparticles were used by us to prepare FeNPs@GO and FeNPs@rGO nanocomposites. Synthesis of graphene oxide. The following chemicals were used: iron chloride, sodium nitrate, potassium permanganate, hydrogen peroxide (30%), sulfuric acid (98%), Ag(NO3)2, NiSO4, ice CO(NO3) and distilled water. The synthesis of FeNPs@GO and FeNPs@rGO was carried out by a modified Hummers–Offerman method [20]. GO and rGO containing iron ions were used to enhance the functional centers. After weighing 3 g of graphite, 1 g of NaNO3 and 6 g of KMnO4 three times, they were placed in a 250 ml graduated cylindrical flask containing 46 ml of 95-98% sulfuric acid (H2SO4). KMnO4 was gradually introduced into the flask over 2 h and then the flask was cooled to 20 °C. The mixture in the flask was cooled in an ice bath. Then the temperature of the flask was lowered to 0 °C. Cooling of the flask was stopped, and the mixture was kept at room temperature until it reached 20 °C. The resulting mixture in the flask was stirred with a stirrer at 20-25 °C for 4 hours. After that, 92 ml of water were added to the mixture over 4 hours. During this time, the temperature of the mixture increased to 90 °C. The temperature of the flask with the mixture was lowered in an ice bath. 280 ml of distilled water were used to wash the reaction products. To increase the degree of oxidation of GO, hydrogen peroxide and iron nanoparticles and/or Fe3O4 were added to the mixture. Composite materials FeNPs@GO and FeNPs@rGO were obtained by layer-by-layer bonding of nanostructured iron with GO nanolayers. Complete interpenetration and distribution of components in the FeNPs@GO and FeNPs@rGO composite occurs within 7 hours. Characterization of samples. The following methods of physicochemical analysis were used to study the properties and establish the arrangement of components in the structure of FeNPs@GO and FeNPs@rGO nanocomposites: X-ray diffraction (XRD), Fourier transform infrared spectroscopy (FTIR), transmission electron microscopy (TEM), chemical analysis. Thus, the structure of FeNPs@GO and FeNPs@rGO, concentration (in particular, FeNPs), type, functional groups (in particular, carbonyl, hydroxyl, ketone and epoxy groups), morphology of the structures of FeNPs@GO and FeNPs@rGO nanocomposite samples were determined.

3. Results and discussion

Figure 1 shows the scheme of graphene oxide reduction. The analysis shows that the developed GO and rGO layers can be used as a membrane. The grain sizes (nm) of the agglomerates (from A to L) in Table 2 correspond to the areas indicated on the TEM surface of the sample (Fig. 2).

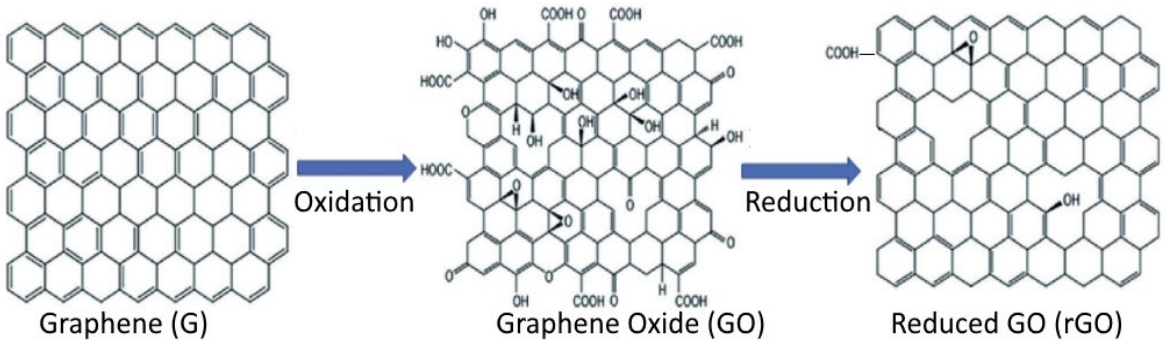

Fig. 1. General scheme of graphene oxide GO reduction.

Fig. 2-6 and the table 1,2 present the results of the physicochemical analysis of the obtained nanoparticles NPs composites based on graphene oxide.

Table 1. Sizes of agglomerations of graphite nanoparticles NPs.

Position	Sizes, nm	Position	Sizes, nm
A	428.6	G	214.3
B	214.3	H	178.6
C	142.8	I	250.0
D	142.8	J	214.3
E	250.0	K	214.3
F	250.0	L	200.0

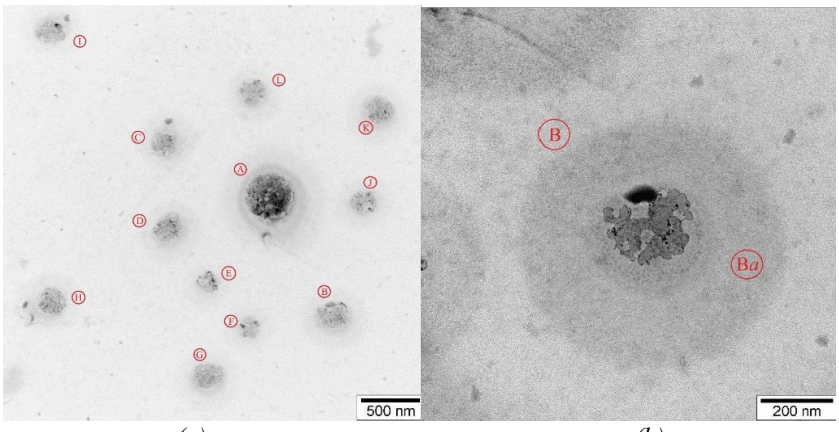

(a) *(b)*

Fig. 2. TEM images of carbon nanoparticles agglomerations (a) Scale - 500 nm, (b) Scale - 200 nm.

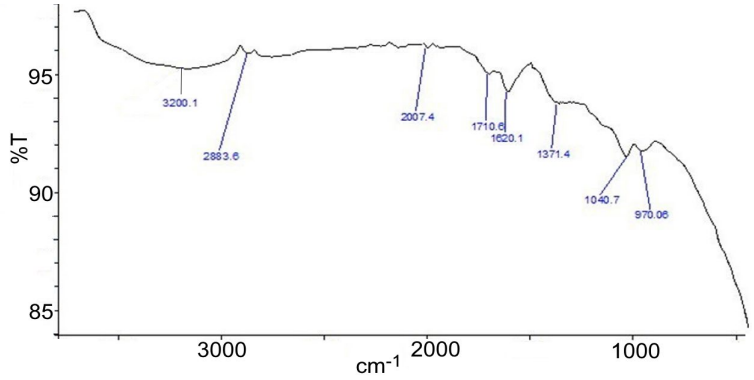

Fig. 3. FTIR result of graphene oxide.

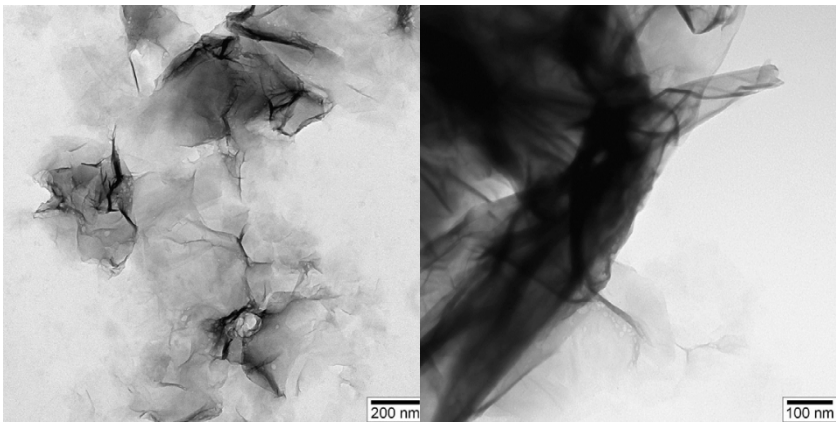

(a) *(b)*

Fig. 4. TEM images of GO. (a) - 200 nm, (b) - 100 nm.

Table 2. FTIR results of GO.

Functional groups		Wavelength, cm^{-1}
OH		3200.1
-C-H		2883.6
C=O		1710.6
C=C		1620.1

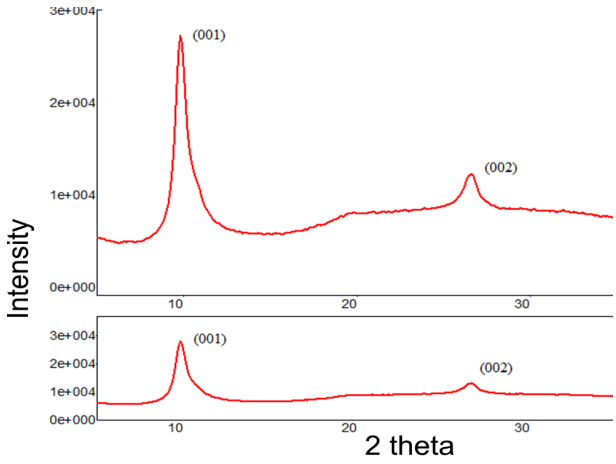

Fig. 5. X-ray diffraction of graphene oxide.

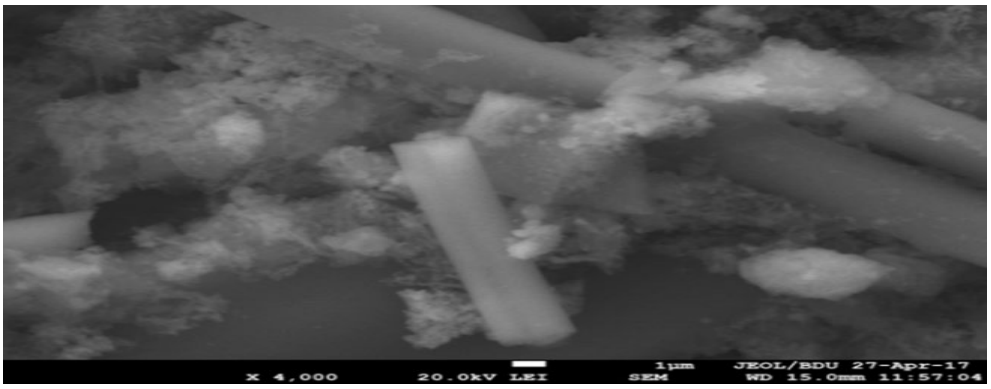

Fig. 6. SEM spectra of stabilised GO NPs.

Tables 3 and 4 present the results of purification of model aqueous solutions at room temperatures using membranes based on FeNPs@GO. The relative error in determining the cation concentration was 3–4%.

Table 3. Concentration of $NiSO_4$ salt in aqueous solution before and after Ni^{2+} purification using FeNPs@GO membrane film.

Concentration (wt.%) of iron nanoparticles in GO	Concentration (wt.%) of $NiSO_4$ salt in aqueous solution before Ni^{2+} purification	Concentration (wt.%) of $NiSO_4$ salt in aqueous solution after Ni^{2+} purification
1	50	13.3
1.1	50	12.9
1.3	50	10.1
1.5	50	8.7
2	50	3.7

Table 4. Concentration of $Co(NO_3)_2$ salt in aqueous solution before and after Co^{2+} purification using FeNPs@GO membrane film.

Concentration (wt.%) of iron nanoparticles in GO	Concentration (wt.%) of $Co(NO_3)_2$ salt in aqueous solution before Co^{2+} purification	Concentration (wt.%) of $Co(NO_3)_2$ salt in aqueous solution after Co^{2+} purification
1	30	9.7
1.1	30	9.3
1.3	30	9.0
1.5	30	7.3
2	30	4.7

During the formation of the membrane material, channels are created that allow the transfer of water molecules in a two-dimensional (2D) structure. Such a 2D structure of GO-based thin films with a thickness of about one atom can prevent the movement of harmful molecules, such as gas molecules and ions of non-aqueous solutions. The formed GO-based thin films with the participation of iron nanoparticles have high mechanical strength and flexibility. Various methods are used to obtain GO, including oxidation of graphite powders (Gt) and then exfoliation of graphite oxide (GtO). The resulting GtO contained hydroxyl and epoxy groups in thin (basal) planes and carbonyl and carboxyl groups at the edges of the surface. These groups are easily dispersed in water or another polar solvent. The prepared colloidal suspensions of GtO in a solvent allow the layers to be separated from each other. Thus, bulk GtO were exfoliated. The GO structure formed from GtO, containing –OH, –COOH, –C–O–C– groups, is hydrophilic and stable. It is known that the formed GO is highly dispersed in aqueous solution. Therefore, it is difficult to separate it from the solution during the production of GO films. By introducing or binding metals and magnetic nanoparticles into the GO structure, the above problem of separating GO from the solution is solved. Magnetic particles bound to GO have high adsorption capacity for harmful cations and pollutants. Thus, graphite oxide (GtO) obtained based on the Hammer method was a precursor for its oxidation. The oxidation of GtO formed a dispersion of GO in an aqueous solvent. The GO dispersions were then deposited as layered structures. The reduction reaction of GO dispersions was carried out with the subsequent formation of reduced rGO. The composites of GO and rGO-based materials were chemically modified using iron nanoparticles FeNPs. Then FeNPs@GO and FeNPs@rGO were used, in particular, as membrane films for water purification from harmful cations. Individual standing layers of FeNPs@GO and FeNPs@rGO have gaps of about 10 nm between the well-packed sheets of the structure. Such composite nanofiltration membranes based on GO have pores smaller than 3 nm. Varying the concentration of FeNPs in GO can change the distance between the nanosheets and modify the structure of FeNPs@GO and FeNPs@rGO. These film membranes have a high level of capture of harmful cations. This is demonstrated by the example of transition cations (Ni^{2+} (r = 0.69 Å) and Co^{2+} (r = 0.74 Å) in aqueous solutions. These membranes based on defect-free FeNPs@GO and FeNPs@rGO with structural stability are recyclable and can compete with large-pore nylon ultrafiltration membranes (pore size 0.22 μm). As follows from the experimental data, the formed nanocomposite membranes based on FeNPs@GO and FeNPs@rGO have a higher cleaning capacity than nanocrystalline GO. The inclusion of FeNPs in the GO structure significantly reduces the pore sizes of GO. This may be due to an increase in surface pressure in nanosized particles and the anisotropy of the elastic properties of FeNPs. Such nanocomposites have high water permeability compared to traditional water purification methods. The different degrees of filtration of GO membranes can be related, for example, to the pore size of the GO structures and the presence of empty spaces between non-oxidizing GO sheets. The presence of hydrophilic groups and fragments at the interfaces of GO surface can change the distance between GO layers and affect the filtration rate of GO-based nanocomposites. Thus, FeNPs@GO and FeNPs@rGO were used as membrane materials and showed significant adsorption properties in water purification. These properties are due to the hydrophilic bonds in GO and rGO, as well as the large surface area of FeNPs@GO and FeNPs@rGO. Oxygen-containing groups of GO and rGO form stable complexes with various

particles and pollutants in solutions. Such complexes facilitate dispersion, in particular, of FeNPs@GO and FeNPs@rGO nanocomposites in aqueous solution. In this work, we did not consider the problem of FeNPs@GO and FeNPs@rGO membrane recovery after using them for cation purification.

4. Conclusions

A set of FeNPs@GO and FeNPs@rGO nanocomposites was synthesized, where iron ions were bound to sheets of graphene oxide GO and reduced rGO. The interactions between the components of the nanocomposites were carried out in aqueous solutions. The final ordered and homogeneous porous structure of the nanocomposites was stable. The concentration of iron nanoparticles in GO-based materials did not exceed 2 wt.% of the total mass of FeNPs@GO and FeNPs@rGO in the composite samples. The incorporation of FeNPs into GO and rGO in one layer ensures uniform distribution of nanoparticles on the surface. This improves the reproducibility of the properties of FeNPs@GO and FeNPs@rGO samples. Functional groups (carboxyl, carbonyl and hydroxyl functional groups) and oxygen atoms are located in different spatial positions of the FeNPs@GO and FeNPs@rGO structures. Nanocomposite membranes containing iron particles provide effective purification of aqueous solutions from harmful cations, such as nickel and cobalt. It was found that the nanocrystalline membranes based on FeNPs@GO and FeNPs@rGO have a higher cleaning capacity than nanocrystalline GO due to a significant decrease in the pore size of the GO structure. The reason for the decrease in pore size with nanocrystalline FeNPs@GO and FeNPs@rGO may be an increase in surface pressure in nanosized particles and anisotropy of the elastic properties of the crystal. Membranes based on FeNPs@GO and FeNPs@rGO have a relatively high-water permeability compared to the GO membrane. At the same time, the ability to retain, for example, harmful cations Ni^{2+} (r = 0.69 Å) and Co^{2+} (r = 0.74 Å) is high. For different samples of aqueous solutions of NiSO4 and Co(NO3)2 salts, the degree of purification was 37-46% and 20-25%, respectively. For different samples of aqueous solutions of $NiSO_4$ and $Co(NO_3)_2$ salts, the degree of purification by NPs@GO membranes was 37-46% and 20-25%, respectively. The high adsorption capacity of the obtained FeNPs@GO and FeNPs@rGO nanocomposites allows them to be recommended as separating membranes for purifying solutions from harmful salt cations.

References

[1] T. Soltani, B. K. Lee, (2016), Chem. Eng. J. 306, 204-213; https://doi.org/10.1016/j.cej.2016.07.051

[2] O. Jankovský, A. Jiříčková, J. Luxa, D. Sedmidubský, M. Pumera, Z. Sofer, (2017), ChemistrySelect 2 9000-9006; https://doi.org/10.1002/slct.201701784

[3] N. A. Guliyeva, R. G. Abaszade, E. A. Khanmammadova, E. M. Azizov, (2023), Journal of Optoelectronic and Biomedical Materials, 15(1), 23 – 30; https://doi.org/10.15251/JOBM.2023.151.23

[4] N. A. Akbarov, N. A. Guliyeva, (2024), International Scientific Journal «Endless Light In Science, 242-245.

[5] N. A. Guliyeva, E. M. Azizov, (2022), International Journal of Sciences: Basic and Applied Research (IJSBAR), 65(1), 141-147.

[6] R. G. Abaszade, (2022), Journal of Optoelectronic and Biomedical Materials, 14(3), 107-114; https://doi.org/10.15251/JOBM.2022.143.107

[7] R. G. Abaszade, S. A. Mammadova, O. A. Kapush, F. G. Agayev, A. M. Nabiev, M. M. Mammadova, S. I. Budzulyak, V. O. Kotsyubynsky, (2021), Physics and Chemistry of Solid State, 23(3), 595-601; https://doi.org/10.15330/pcss.22.3.595-601

[8] S. R. Figarova, E. M. Aliyev, R. G. Abaszade, R. I. Alekberov, V. R. Figarov, (2021); Journal of Nano Research, 67, 25-31; https://doi.org/10.4028/www.scientific.net/JNanoR.67.25

[9] R. G. Abaszade, A. G. Mammadov, I. Y. Bayramov, E. A. Khanmamadova, V. O. Kotsyubynsky, O. A. Kapush, V.M.Boychuk, E.Y.Gur, (2022), Physics and Chemistry of Solid State, 25(2), 256-260; https://doi.org/10.15330/pcss.23.2.256-260

[10] R. G. Abaszade, A. G. Mammadov, I. Y. Bayramov, E. A. Khanmamadova, V. O. Kotsyubynsky, E. Y. Gur, O. A. Kapush, (2022), Technical and Physical Problems of Engineering, 14(2), 302-306.

[11] V. M. Boychuk, R. I. Zapukhlyak, R. G. Abaszade, V. O. Kotsyubynsky, M. A. Hodlevsky, B. I. Rachiy, L. V. Turovska, A. M. Dmytriv, S. V. Fdorchenko, (2022), Physics and Chemistry of Solid State, 23(2), 815-824; https://doi.org/10.15330/pcss.23.4.815-824

[12] S. R. Figarova, E. M. Aliyev, R. G. Abaszade, V. R. Figarov, (2023), Advanced Materials Research, 1175, 55-62; https://doi.org/10.4028/p-rppn12

[13] R. G. Abaszade, A. G. Mammadova, E. A. Khanmammadova, I. Y. Bayramov, R. A. Namazov, Kh. M. Popal, S. Z. Melikova, R. C. Qasımov, M. A. Bayramov, N. I. Babayeva, (2023), Journal of Ovonic Research, 19(2), 259-263; https://doi.org/10.15251/JOR.2023.193.259

[14] B. Sharma, A. Singh, A. Sharma, A. Dubey, V. Gupta, R. G. Abaszade A. K. Sundramoorthy, N. Sharma, S. Arya, (2024), Applied Physics A 130:297; https://doi.org/10.1007/s00339-024-07472-0

[15] N. Ivanichok, P. Kolkovskyi, O. Ivanichok, V. Kotsyubynsky, V. Boychuk, B. Rachiy, M. Bembenek, Ł. Warguła, R. Abaszade, L. Ropyak, (2024), Materials, 17(2514), 1-21; https://doi.org/10.3390/ma17112514

[16] M. M. Ramazanov, A. M. Maharramov, S. F. Hajiyeva, Y. V. Parfyonova, G. M. Eyvazova, F. V. Hajiyeva, N. A. Guliyeva, (2016), J. of Nanotechnology in Engineer. and Medicine, 6(4); https://doi.org/10.1115/1.4033126

[17] P. Tancredi, L. O. Moscoso, R. Rivas, C. Patricia, M. Knobel, M. L. Socolovsky, (2018), Materials Research Bulletin, S0025540818305415; https://doi.org/10.1016/j.materresbull.2018.08.003

[18] S. Zhu, J. Guo, J. Dong, Z. Cui, T. Lu, C. Zhu, D. Zhang, J. Ma, (2013), Ultrasonics Sonochemistry, 20 872-880; https://doi.org/10.1016/j.ultsonch.2012.12.001

[19] H. P. Cong, J. J. He, Y. Lu, S. H. Yu, (2010), Small, 6 169-173; https://doi.org/10.1002/smll.200901360

[20] W. S. Hummers, R. E. Offerman, (1958), Journal of the American Chemistry Society, 80 1339-1339; https://doi.org/10.1021/ja01539a017

[21] S. Eigler, M. Enzelberger-Heim, S. Grimm, P. Hofmann, W. Kroener, A. Geworski, C. Dotzer, M. Rockert, J. Xiao, C. Papp, O. Lytken, H. P. Steinruck, P. Muller, A. Hirsch, (2013), Wet chemical synthesis of graphene, Advanced Materials, 25 3583-3587; https://doi.org/10.1002/adma.201300155

[22] X. Hong, X. Wang, Y. Li, J. Fu, B. Liang, (2020), Catalysts, 10, 921; https://doi.org/10.3390/catal10080921

[23] S. Zhang, B. Li, X. Wang, G. Zhao, B. Hu, Z. Lu, T. Wen, J. Chen, X. Wang, (2020), Chemical Engineering Journal, 390, 124642; https://doi.org/10.1016/j.cej.2020.124642

[24] C. D. Marcano, V. D. Kosynkin, M. J. Berlin, S. A. Sinitskii, A. S. Zhengzong, B. L. Alemany, W. Lu, M. J. Tour, (2010), ACS Nano. 4(8), 4806-4814; https://doi.org/10.1021/nn1006368

[25] V. A. Labunov L. V. Tabulina, P. Yu. Shaman, I. V. Komissarov, T. G. Rusalskaya, M. V. Silibin, A. V. Sysa, (2020), Method for producing graphene oxide. Patent 036651 B1; application number 201800459; Application filing date 2018.07.18; Patent publication and issue date 2020.12.04.

[26] A. M. Dimiev, S. Eigler, (2017), Graphene Oxide: Fundamentals and Applications, 1st ed.; John Wiley & Sons: Hoboken, NJ, USA, 454. https://doi.org/10.1002/9781119069447

[27] G. D. Trikkaliotis, K. A. Christoforidis, C. Athanasios, (2021), ChemEngineering 5, 64; https://doi.org/10.3390/chemengineering5030064

[28] R.G.Abaszade, M.B.Babanli, V.O.Kotsyubynsky, A.G.Mammadov, E.Gür, O.A.Kapush, M.O.Stetsenko, R.I.Zapukhlyak, (2023), Physics and Chemistry of Solid State, 24(1), 53-158; https://doi.org/10.15330/pcss.24.1.153-158